

# Do triangles matter? Replicating hypergraph disease dynamics with lower-order interactions

Eugene Tan\*

*The Kids Research Institute Australia, Nedlands 6009, Australia<sup>†</sup>*

Michael Small<sup>‡</sup> and Shannon D. Algar<sup>§</sup>

*The Complex Systems Group, The University of Western Australia, Crawley 6009, Australia*

(Dated: August 29, 2025)

Disease spreading models such as the ubiquitous SIS compartmental model and its numerous variants are widely used to understand and predict the behaviour of a given epidemic or information diffusion process. A common approach to imbue more realism to the spreading process is to constrain simulations to a network structure, where connected nodes update their disease state based on pairwise interactions along the edges of their local neighbourhood. Simplicial contagion models (SCM) extend this to hypergraphs such that groups of three nodes are able to interact and propagate the disease along higher-order hyperedges (triangles). Though more flexible, it is not clear the extent to which the inclusion of these higher-order interactions result in dynamics that are characteristically different to those attained from simpler pairwise interactions. Here, we propose an agent-based model that unifies the classical SIS/SIR compartmental model and SCM, and extends it to allow for interactions along hyperedges of arbitrary order. Using this model, we demonstrate how the steady-state dynamics of pairwise interactions can be made to replicate those of simulations that include higher-order topologies by linearly scaling disease parameters based on a proposed measure network activity. By allowing disease parameters to dynamically vary over time, lower-order pairwise interactions can be made to closely replicate both the transient and steady-state dynamics of higher-order simulations.

## INTRODUCTION

Spreading processes over a given topology are ubiquitous across many social and physical systems. From epidemics to information diffusion, many studies aim to understand the governing rules of spreading processes in social contexts. Spanning topics such as disease epidemics [1, 2]. Nevertheless, the influence of the underlying topology on which spreading occurs can sometimes be as important as the mechanistic rules governing the spreading process [3, 4]. This consideration is crucial in the study of contagion and epidemics on social networks, where local properties like degree and clustering can mediate non-trivial dynamics such as super-spreader events and endemic states [4, 5].

Recent approaches propose the inclusion of interactions along higher-order topologies such as simplices (e.g. triangles, tetrahedrons) to account for social interactions that include more individuals than pairwise interactions. The inclusion of higher-order interactions have been shown to promote critical transitions and bistability in epidemics [6–8]. However, the importance that they play in altering the overall epidemic trajectory is less clear.

In this Letter, we present a discrete numerical model that generalises the classical SIS/SIR compartmental model with homogeneous mixing to account for hyper-edge interactions of arbitrary order. Comparing dynamics with and without higher-order interactions, we find topology primarily affects epidemic transients. If the network structure is known, one can calculate normalisation

values related to the potential network activity. These values may be used to define disease parameters for first-order pairwise interactions that replicate the steady state dynamics of those that include higher-order interactions, but are insufficient for reproducing epidemic transients. However, we find a duality where the effects of network topology can be overcome by allowing for temporally varying disease parameters; allowing first-order dynamics to closely approximate both transient and steady state trajectories of higher-order systems. Whilst the calculation of normalisation values requires knowledge of the order scaling of interaction dynamics, we show robustness to model misspecification provided the relative size scales between interaction orders are comparable. These results are broadly aligned with the recent analytical results by [9] where mean field approximations of pairwise interactions were able to capture features of simplicial contagion

## DISEASE MODEL

We begin by presenting a variation of the classical compartmental ODE model [9] focusing on the three compartment case with susceptible-infected-removed (SIR) states,

$$\frac{dS}{dt} = -\beta SI + \mu I, \quad \frac{dI}{dt} = \beta SI - \mu I - \alpha I, \quad \frac{dR}{dt} = \alpha I \quad (1)$$

where  $N = S + I + R$  is the total population and  $S, I, R$  are the susceptible, infected and removed populations re-

spectively. The constants  $\beta$ ,  $\mu$  and  $\alpha$  are disease parameters corresponding to the rates of infection, recovery and removal. For  $\alpha = 0$ , the SIR system reduces to the simpler SIS system.

The simple SIR model assumes that populations homogeneously mix. However, this is not true for human populations where disease spread occurs on a social contact network. Here, individuals – represented as nodes – interact within a small neighbourhood with occasional branching, clustering or long range connections [3, 10, 11]. One can simulate more realistic spread dynamics by employing an agent-based approach where randomly selected nodes interact with all or a collection of their neighbours every time step [12]. Whilst this node-based approach is more realistic for modelling the diffusion of abstract quantities such as information, it is not necessarily adequate for disease contagion as it treats individuals rather than interactions as facilitators of infection. It is unlikely for an individual to interact with all of their neighbours in a given time step. Instead, we propose simulating diseases on networks using an edge-based approach.

Let  $G = (E, V)$  be a hypergraph consisting of a set of hyperedges  $E$  and nodes  $V$ . A  $k^{th}$  order hyperedge is a connection between  $k+1$  different nodes. Each simulation time step consists of  $m$  iterations. A random hyperedge  $e \in E$  is selected in each iteration. Each susceptible node  $s_i$  in  $e$  has a probability  $\beta_e$  of getting infected and transitioning to state  $I$ ,

$$\beta_e = \min \left[ f \left( \frac{n_I(e)}{n_S(e) - 1} \right) n_I(e) \beta_{ABM}, 1 \right], \quad (2)$$

where  $n_I(e)$  and  $n_S(e)$  are the number of nodes in  $e$  that are infected and susceptible respectively,  $\beta_{ABM}$  is a base infection probability for a pairwise interaction, and  $f$  is a scaling function that controls the extent to which multiple infected nodes in a given hyperedge amplify the probability of infection. In simplicial social contagion models (SCM) where interactions occur up to order  $k = 2$ , susceptible nodes whose neighbours are all infected experience an amplified probability of infection [3]. Whilst it has only been applied to social dynamics (e.g. knowledge spreading), we argue that a similar principal is also relevant when studying diseases where the infection probability may be mediated by the concentration of disease particles within an individual's immediate vicinity during an interaction. The allowance for variable infectivity with has been explored prior by Fu et al. [13]. Inspired by this, we use the following scaling function to describe the disease spread dynamics on hyperedges,

$$f(p) = \begin{cases} 2p, & 0 \leq p < 0.5 \\ 1 + 2k_\gamma(2p - 1), & p \geq 0.5 \end{cases} \quad (3)$$

where  $k_\gamma$  is the maximum amount that a hyperedge interaction can amplify the infection probability. After inter-

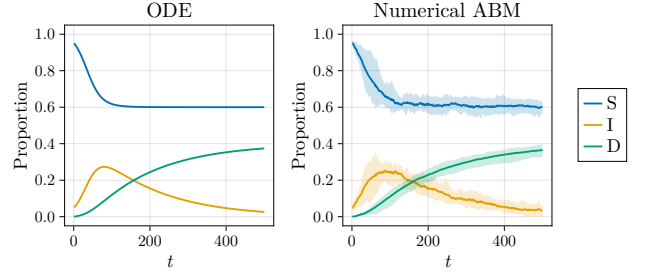


FIG. 1. Epidemic trajectories from ODE model assuming homogeneous mixing, and 20 simulations of the numerical approximation using a  $N = 500$  node fully connected network. Mean and 90% quantiles shown. Parameters are  $\beta_{ODE} = 0.0003$ ,  $\mu_{ODE} = 0.5N\beta_{ODE}$ ,  $\alpha_{ODE} = 0.04N\beta_{ODE}$ .

action, all infected nodes recover or die with probabilities  $P(I \rightarrow S) = \mu_{ABM}$  and  $P(I \rightarrow R) = \alpha_{ABM}$ .

The proposed numerical model achieves two goals. Firstly, it unifies the classical homogeneous ODE disease model with existing SCM up to order  $k_{max} = 2$ . For  $k_{max} = 1$  and a fully connected graph  $G$ , this model is a numerical approximation for the SIR/SIS model using the following disease parameters,

$$\beta_{ABM} = \frac{N(N-1)}{2} \beta_{ODE} \delta t, \quad (4a)$$

$$\mu_{ABM} = \mu_{ODE} \delta t, \quad (4b)$$

$$\alpha_{ABM} = \alpha_{ODE} \delta t, \quad (4c)$$

where  $\delta t = 1/m$  is the integration time step. We validate simulations against the analytical ODE model and find good agreement in epidemic trajectories (see Fig. 1). For  $k_{max} = 2$ , the model is equivalent to an edge-based formulation of the simplicial contagion model (SCM) by Iacopini et al. [3], with the conversion,

$$k_\gamma = \frac{\beta + \beta_\Delta}{2\beta}, \quad (5)$$

where  $\beta_\Delta$  is the simplicial infection rate. Secondly, this generalises simplicial contagion to account for simplices of arbitrary order and varying proportions of infected individuals within each hyperedge.

## NETWORK ACTIVITIES

Identifying dynamical differences between networks with and without interactions on higher-order topologies requires an appropriate normalisation that allows for comparison. Thus, we consider two candidate quantities related to the rate of new infection  $\frac{dI}{dt}$ .

The first quantity, called the combinatorial network activity  $\hat{\lambda}^{(K)}$  calculated up to order  $K$  for a hypergraph  $G$  with respect to a baseline infection rate  $\beta$  is defined

as,

$$\hat{\lambda}^{(K)}(G, \beta) = \frac{\sum_{k=1}^K N_k \hat{\beta}^{(k)}}{\sum_{k=1}^K N_k}, \quad (6)$$

where

$$\hat{\beta}^{(k)} = \frac{\sum_{i=0}^{k+1} \binom{k+1}{i} (k+1-i) \min[f(\frac{i}{k}), \beta, 1]}{\sum_{i=0}^{k+1} \binom{k+1}{i}}, \quad (7)$$

and approximates  $\frac{dI}{dt}$  under the assumption that individuals are equally likely to be infected or susceptible. Therefore,  $\hat{\lambda}^{(K)}$  depends only on network the network topology and the scaling function  $f$ .

Similarly, an exact network activity  $\lambda^{(K)}$  up to order  $K$  can be calculated as,

$$\lambda^{(K)}(G, \beta, X) = \frac{\sum_{e \in E_K} n_S(e) \beta_e}{|E_K|}, \quad (8)$$

where  $E^{(K)}$  is the set of all hyperedges of order up to  $k_{max} = K$ , and  $X$  are the nodes' states. Unlike the  $\hat{\lambda}^{(K)}$ ,  $\lambda^{(K)}$  does not assume a distribution of node states and is instead a function of the full network state and approximates the instantaneous value of  $\frac{dI}{dt}$ .

## RESULTS

To identify the role of higher-order interactions in disease spreading dynamics, we pose the following question: Can pairwise interactions replicate higher-order dynamics using an appropriate normalisation?

We address this question using the case of SIS dynamics with baseline disease parameters  $(\beta, \mu, \alpha) = (0.05, 0.0001, 0)$ . The SIS case is analysed first as it possesses steady states on which measures can be defined. We later extend our analyses to the more general SIR case.

Given an undirected  $N$  node network with a pairwise adjacency matrix  $A$ , we define two different hypergraphs  $G_1 = (E_1, V)$ , and  $G_K = (E_K, V)$  with hyperedges defined up to the order 1 and  $K$  clique complex of  $A$  respectively. Parallel simulations with the same initial conditions are conducted using disease parameters  $(\beta_1, \mu, \alpha)$  and  $(\beta_K, \mu, \alpha)$  with infection values normalised using the ratio of both networks' combinatorial network activity,

$$\beta_1 = \frac{\hat{\lambda}^{(K)}(G_K, \beta)}{\hat{\lambda}^{(1)}(G_1, \beta)} \beta_K, \quad (9a)$$

$$\beta_K = \beta. \quad (9b)$$

This normalisation ensures that simulations on both  $G_1$  and  $G_K$  begin with approximately similar network activity. Thus, deviations in the epidemic trajectories of both simulations are the result of topology rather than disease parameters.

This test is run on two  $N = 500$  node networks with different topologies: a 2D triangular lattice, and an Erdős-Rényi (ER) random network with connection probability  $p = 0.1$ . The triangular lattice represents the case where the probability of higher order interactions is greatest (i.e.  $\frac{|E_K|}{|E_1|}$  is maximised) for  $K = 2$ . The random network is the case that allows for multiple orders of interaction, with maximum order chosen to be  $K = 4$ . We run 50 and 10 simulations of the triangular lattice and random network respectively with a resolution of  $m = 50$  (see Fig. 2).

A base case with unnormalised infection rates is run as a control. Enabling higher-order interactions after the pairwise system settles pushes the steady state align with the higher-order scenario. For the test case, applying a normalisation based on the ratio of each network's combinatorial network activity results in epidemic trajectories whose steady state in the  $K = 1$  case closely mimic those of  $K > 1$ . However, the initial adjustment of disease parameters is insufficient for replicating epidemic transients in earlier portions of the trajectory. These findings suggest that network topology and higher-order interactions are critical during epidemic transients, but washes out in the endemic steady state. In early stages of the epidemic, infection spread is primarily mediated by the local network structures in the neighbourhood of infected agents, which in turn govern the slopes of the trajectory. Once steady state is achieved, pairwise first-order  $K = 1$  interactions given an appropriate normalisation is sufficient to reproduce spread dynamics.

The above finding naturally leads the discussion to a second question: Under what minimal conditions can pairwise interactions be used to replicate those of higher-order? We again perform similar tests consisting of two parallel simulations with separate disease parameters with the exception that the infection rate of the  $K = 1$  case is allowed to vary over time, with parameters  $(\beta_1(t), \mu, \alpha)$  and  $(\beta_K, \mu, \alpha)$ . This is plausible in cases where disease strains evolve, or intervention policies are enforced (i.e. dynamic network structures, altered infection parameters).

For simulating adaptive disease parameters, we first calculate the moving average of the exact network activity ratios in both hypergraphs,

$$\xi(t) = \frac{\lambda^{(K)}(G_K, \beta, X_K(t))}{\lambda^{(1)}(G_1, \beta_1(t), X_1(t))}, \quad \bar{\xi}(t) = \frac{1}{\tau} \sum_{n=t}^{t+\tau} \xi(n), \quad (10)$$

where  $\tau = 5$  a set window length. The pairwise infection rate parameter  $\beta_1(t)$  is dynamically adjusted with respect to a conservative set threshold  $\rho = 0.5$

$$\beta_1(t) = \begin{cases} \beta_1(t-1), & |\bar{\xi}(t) - 1| < \rho \\ \xi(t) \beta_1(t-1), & |\bar{\xi}(t) - 1| \geq \rho \end{cases} \quad (11)$$

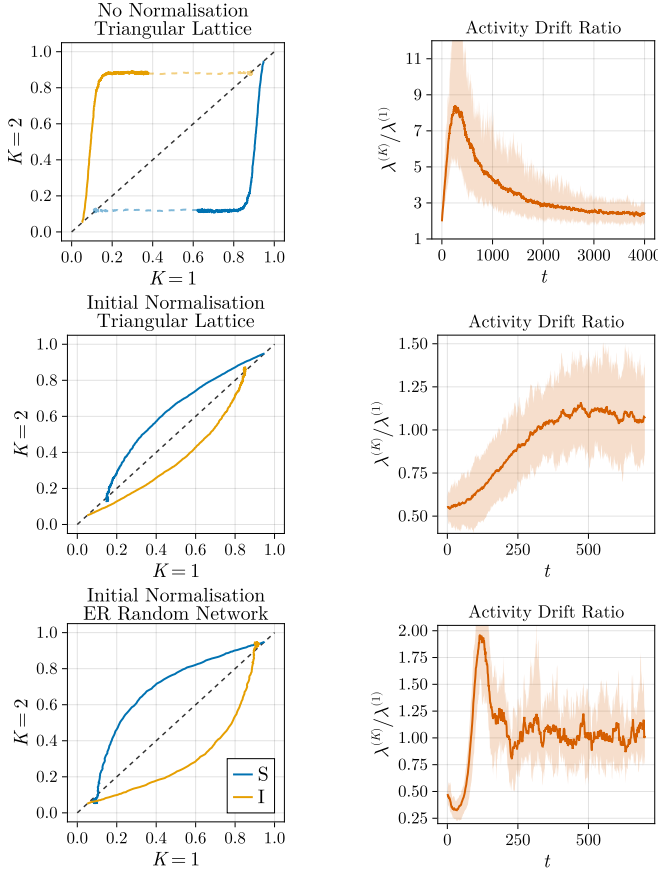


FIG. 2. SI epidemic trajectories between the pairwise and higher-order simulations. Accompanying activity ratios are shown right revealing a saturation to 1 as the epidemic reaches the endemic steady state. Dotted trajectory in the unnormalised case corresponds to enabling of higher-order interactions in pairwise simulation.

The adjustment of  $\beta_1(t)$  based on a threshold of the moving average  $\xi(t)$  limits the extent to which the infection parameter is allowed to vary, and thus aims to mimic a more realistic evolution of disease dynamics where base infection rates are less volatile.

Results for the normalisation tests with dynamically varying disease parameters are shown in Fig. 3. We find that the dynamical adjustment of disease parameters allows for first-order (pairwise) simulations to replicate those of higher order in both transient and steady state regimes. Furthermore, we note that the adjustments of disease parameters are infrequent, with 2-4 adjustment events occurring across 700 simulated time steps in each simulation. A majority of adjustments occur during the first half of the transient regime. These results suggest a duality between network topology and disease parameters. Namely, the effects of higher-order interactions may be partially accounted for in first-order approximations through the presence of dynamic disease parameters.

To test the robustness of this result, the same numer-

ical experiment is repeated using a misspecified scaling function  $\hat{f}(p)$  when calculating activity ratios  $\xi$ . We test two types of misspecification: scale  $\hat{f}_1(p)$ , and functional form  $\hat{f}_2(p)$  given by,

$$\hat{f}_1(p) = \begin{cases} 2p, & 0 \leq p < 0.5 \\ 1 + 2k_\gamma\eta(2p - 1), & p \geq 0.5 \end{cases} \quad (12a)$$

$$\hat{f}_2(p) = \begin{cases} (2p)^{1/n}, & 0 \leq p < 0.5 \\ 1 + 2k_\gamma(2p - 1)^n, & p \geq 0.5 \end{cases} \quad (12b)$$

The parameter  $\eta$  controls the misspecification in the amplification infection rates due to higher-order interactions, and  $n$  affects the degree of nonlinearity from the true scaling function  $f(p)$  (see Fig. 4).

We simulate disease dynamics for trajectory pairs of  $K = 1$  and  $K = 4$  on a 500 node ER random network for  $\eta \in \{0.5, 0.8, 1.2, 1.5, 2\}$  and  $n \in \{2, 3, 4, 5\}$ . In both cases, dynamic normalisation of infection rates based on network activity ratios calculated with  $\hat{f}_1, \hat{f}_2$  remained sufficient for pairwise interactions to replicate trajectories from simulations that include higher-order interactions (see Fig. 4). We observe that scale errors are more detrimental to the accuracy of the normalisation errors.

All of the above tests focus on the SIS disease scenario, which is characterised by an epidemic transient followed by a steady state regime where the disease is either eradicated or remains in endemic. For a final validation, we extend our analyses to the SIR case where for suitably chosen disease parameters, infection trajectories exhibit a single peak during the epidemic's transient phase. The same dynamic adjustment for infection rates is applied across a range of base disease parameter values  $\beta_K \in [0.004, 0.08]$  and  $\mu_K \in [0.000025, 0.0005]$  with maximum order  $K = 4$  and  $k_\gamma = 3$ . Phaseplots of the peak time, and peak and final proportions are given in Fig. 5. Overall, we find that normalisations using activity ratios enable higher-order interaction dynamics to be replicated by those of lower order.

## CONCLUSION

In this work, we attempt to quantify the effect of higher-order topologies on the spreading dynamics on networks. Focusing on the single disease case, we have presented an agent-based model that unifies the classical compartmental SIR model of homogeneous mixing with pairwise simplicial contagion models on networks, and extends it to account interactions on hyperedges of arbitrary order. We use this model in conjunction with a normalisation method based on the notion of network activity to compare spread dynamics across hypergraphs of different maximal orders.

The inclusion of higher-order topology is found to primarily affect the transient dynamics in epidemic trajec-

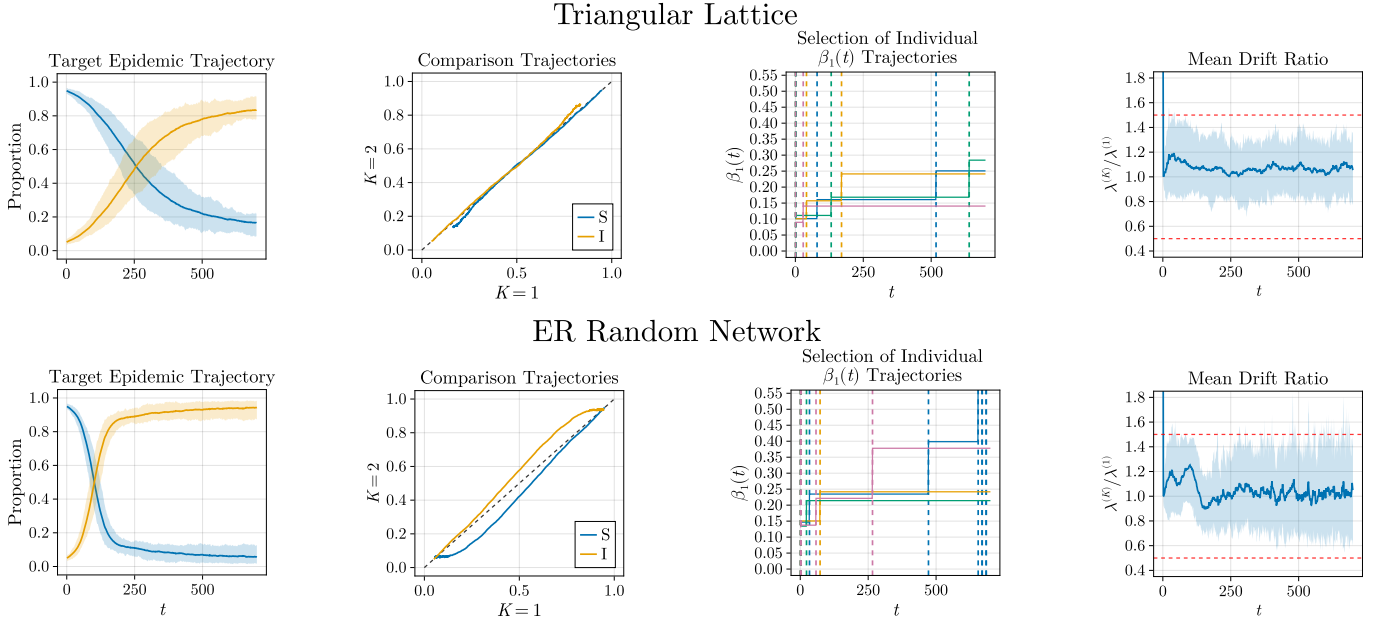


FIG. 3. Simulations with dynamic disease parameters with  $K = 1$  for triangular lattice and random networks. Shaded regions correspond to 90% CI. Left to right: target trajectories from the higher order simulation, comparison trajectories between pairwise and higher order case, four randomly chosen trajectories of  $\beta_1(t)$  with adjustment events indicated by vertical lines, and the mean drift ratio  $\bar{\xi}(t)$ , with the  $\rho$  threshold envelope in red.

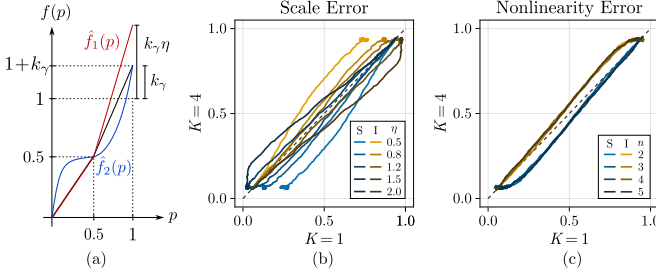


FIG. 4. Schematic of (a) scaling function  $f(p)$  and misspecified forms  $\hat{f}_1(p)$  and  $\hat{f}_2(p)$ . (b) and (c) Comparison trajectories showing robust performance.

tories. Using carefully chosen disease parameters such that initial network activities are approximately equal, simulations restricted to pairwise (order 1) interactions are able to replicate the steady state behaviours resulting from higher-order interactions. Furthermore, a sufficiently accurate normalisation can be calculated purely based on the network topology and the scaling function describing the higher-order interaction. We find that allowing disease parameters to dynamically vary over time is sufficient for pairwise simulations to reproduce full trajectories of higher-order interactions. Thus we conclude that there is a duality between topological effects, and the stationarity of disease parameters.

The ability for pairwise interaction models to reproduce epidemic trajectories from models containing higher-order complexity features raises interesting ques-

tions on the need for higher-order features to be included in disease models. Furthermore, it encourages a reconsideration of whether dynamics, observed or modelled, should be attributed as the result of complex topological structure or temporally varying spreading mechanisms. The above tests focus on epidemic trajectories, which represent summaries of the disease averaged across the entire network. These results invite further questions on the similarity of spreading dynamics on the local scale of a given network and if the order of infection events between individuals differ between interactions of different order. One can also consider the effect of incubation and immunity refractory periods, which may impart a form of time delay in the infection process resulting in more dynamic disease parameters. On application, network activities offer a potential way to construct adaptive rewiring strategies that can be used to maintain a sustainable level of infection.

\* Also at The Complex Systems Group, The University of Western Australia.

† eugene.tan@thekids.org.au

‡ michael.small@uwa.edu.au

§ shannon.algar@uwa.edu.au

- [1] R. Pastor-Satorras, C. Castellano, P. Van Mieghem, and A. Vespignani, Epidemic processes in complex networks, *Reviews of Modern Physics* **87**, 925 (2015).
- [2] M. Jalili and M. Perc, Information cascades in complex networks, *Journal of Complex Networks* **5**, 665 (2017).

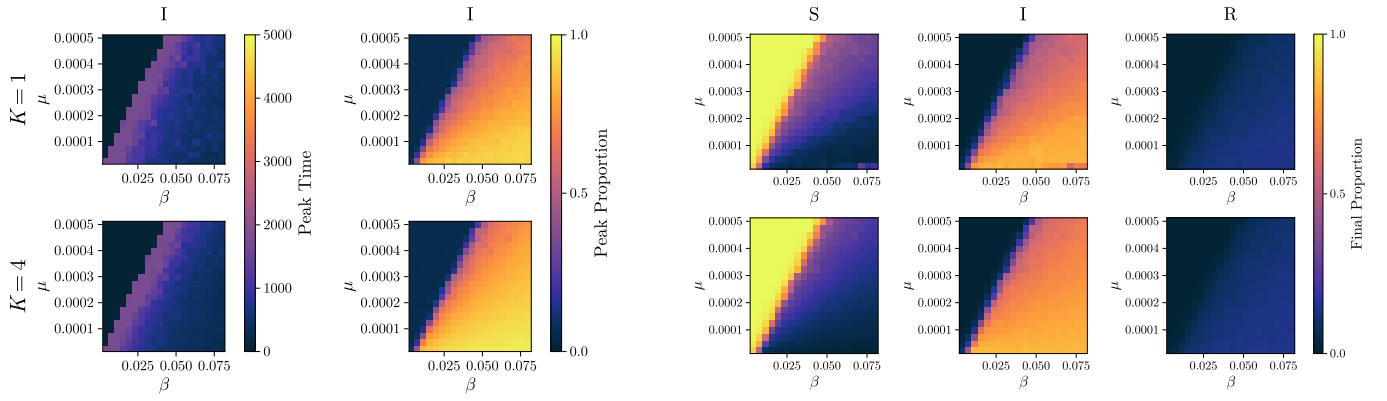


FIG. 5. Phaseplots of the peak time, and peak and final proportions for simulated SIR model with dynamic disease parameters. Top and bottom rows correspond to the pairwise  $K = 1$  and higher-order  $K = 4$  simulations for  $N = 500$  node ER random network. Dynamic adjustment shows good replication of phaseplots and epidemic outbreak threshold.

- [3] I. Iacopini, G. Petri, A. Barrat, and V. Latora, Simplicial models of social contagion, *Nature Communications* **10**, 2485 (2019).
- [4] M. D. Shirley and S. P. Rushton, The impacts of network topology on disease spread, *Ecological Complexity* **2**, 287 (2005).
- [5] M. Small, C. K. Tse, and D. M. Walker, Super-spreaders and the rate of transmission of the SARS virus, *Physica D: Nonlinear Phenomena* **215**, 146 (2006).
- [6] L. Zhao, H. Wang, H. Yang, C. Gu, and J. M. Moore, Susceptible-infected-recovered-susceptible processes competing on simplicial complexes, *Physical Review E* **110**, 064311 (2024).
- [7] M. Lucas, I. Iacopini, T. Robiglio, A. Barrat, and G. Petri, Simplicially driven simple contagion, *Physical Review Research* **5**, 013201 (2023).
- [8] Á. Bodó, G. Y. Katona, and P. L. Simon, SIS epidemic propagation on hypergraphs, *Bulletin of Mathematical Biology* **78**, 713 (2016).
- [9] W. O. Kermack and A. G. McKendrick, A contribution to the mathematical theory of epidemics, *Proceedings of the Royal Society of London. Series A* **115**, 700 (1927).
- [10] S. Boccaletti, P. De Lellis, C. Del Genio, K. Alfaro-Bittner, R. Criado, S. Jalan, and M. Romance, The structure and dynamics of networks with higher order interactions, *Physics Reports* **1018**, 1 (2023).
- [11] I. Z. Kiss, J. C. Miller, and P. L. Simon, *Mathematics of Epidemics on Networks: From Exact to Approximate Models*, Vol. 46 (Springer, 2017).
- [12] R. Pastor-Satorras, A. Vázquez, and A. Vespignani, Dynamical and correlation properties of the internet, *Physical Review Letters* **87**, 258701 (2001).
- [13] X. Fu, M. Small, D. M. Walker, and H. Zhang, Epidemic dynamics on scale-free networks with piecewise linear infectivity and immunization, *Physical Review E* **77**, 036113 (2008).